Effects of the Subtropical Anticyclones over North Africa and Arabian Peninsula on the African Easterly Jet

By James Spinks, email: jspin881@hotmail.com and Dr. Yuh-Lang Lin, email: ylin@ncat.edu

The African easterly jet (AEJ) is a prominent large scale feature over North Africa, which presents a localized zonal wind maximum of about 12 m/s near 600 mb. Several questions regarding the roles played by the AEJ contributing to North African climate and weather have been raised in the past. A number of studies have been devoted to achieving a better understanding of the formation and maintenance of the AEJ, but most of the research has been done in West Africa. Very few studies of AEJ are focused on East Africa, which is the focus of this study.

In this study we will address the AEJ and its two wind maximums over East Africa, West North Africa and the Arabian Peninsula for 32 years of August between 1979 and 2010. We will also explore the dynamics of the Saharan and Arabian highs, and why the East Local Wind Maximum (denoted as LWM_E hereafter) is weaker than the West LWM (denoted as LWM_W hereafter). August was chosen because it is the peak rainfall month over East Africa.

1. BACKGROUND

The AEJ is located in between the dry Saharan and moist tropical regions. The AEJ lies between 600 and 700 mb and exists as a result of the positive meridional temperature gradient (Cook 1999, Thorncroft and Blackburn 1999, Parker et al. 2005, Cornforth et al. 2009). Grist et al. (2002) observed the mean speed of the LWM_W for the month of August to be 10 to 12 m s^{-1}. Another observation was from the Jet2000 project (Thorncroft et al., 2003) that examined the LWM_W to have a much stronger zonal speed of 21 m s^{-1}, which was higher than the climatological average value of 15 m s^{-1} (e.g., Reed et al., 1977). Dezfuli and Nicholson (2010) observed the LWM_W to have a mean speed of 13.5 m s^{-1} and the LWM_E to have a mean speed of 12.7 m s^{-1}.

Chen (2005) described the role that the Saharan high plays on the LWM_W intensity by observing the circulation patterns over Africa. The lower-tropospheric monsoon southerly flow over West Africa is established by the lower branch of the Hadley circulation. The TEJ in the upper troposphere is located aloft over the upward branch of the Hadley circulation, while the LWM_W is placed over the downward branch of the Saharan circulation**.** The upward (hot) vertical motion driven by the thermal low heating and the downward (cold) branch of the Indian monsoon form a strong divergence center. The link between the upper and lower tropospheric circulation over North Africa can be established through this divergence center.

2. DATA

In this study, we will use the ECMWF-Intermediate (ERA-I) reanalysis data with a spatial resolution of 0.75° x 0.75° global for the month of August between 1979 and 2010 (Dee et al. 2011). The investigation of the AEJ structure and intensity from previous studies that used the NCEP reanalysis or the ERA-40 may vary from this research. Limitations of the NCEP data and ERA-40 would include their lower spatial resolution and the discrepancies of the AEJ intensity.

3. RESULTS

4.1 Synoptic Features and Circulation over North Africa

To explore the circulation of subtropical anticyclones, we use streamfunction as a diagnostic variable. For the month of August between 1979 and 2010, the major atmospheric features are depicted in Fig. 1. As seen in Fig. 1a, the TEJ axis is located on the southern rim of the Tibetan high with the TEJ intensity decreasing from east to west. The maximum intensity of the TEJ is located to the south of the Tibetan anticyclone center and extends into the southwestern Arabian Peninsula and East Africa.

At 600 mb (Fig. 1b), two high pressure systems are shown: the Saharan high around (10°W, 25°N) and the other is the Arabian high around (40°E, 25°N). The AEJ axis is located to the south of the anticyclonic circulations around (17°W-45°E, 10°N-20°N). The intensity of the LWM_E at (35°E, 15°N) has a zonal wind speed average of -9.81 m s^{-1} and the intensity of the LWM_W at (17°W, 18°N) has a zonal wind speed average of -13.41 m s^{-1}. Note that the LWM_W and Saharan high are much stronger than the corresponding LWM_E and Arabian high.

At 925 mb, two major anticyclonic systems are located over the Atlantic and Indian Oceans. In Fig. 1c, the Intertropical Front (ITF) can be depicted using upward motion ($-\omega<0$) where there is strong baroclinicity along the convergence zone. Across North Africa at 20°N, the converging winds from the Guinea Monsoon and the northerly Harmattan flow are effects from the generation of the Saharan thermal low (15°W, 20°N). Several intense upward motion regions exist across North Africa as part of the ITF heating. There is a strong vertical motion on the lee side of the Darfur Mountains around (20°E, 20°N), on the lee side of the northern most part of the Ethiopian Highlands around (35°E, 20°N), and another over the Asir Mountains around (43°E, 20°N). The intense vertical motion over the Arabian Peninsula is associated with the Arabian thermal low.

Exploring the east-west circulation will provide insight on how the anticyclonic systems are maintained. The streamlines on a zonal and meridional vertical cross section of North Africa depicts the east-west circulation (Fig. 2a) along the ITF approximately 20°N, the north-south Hadley Circulation over West Africa (10°W-15°W) (Fig. 2b), and the north-south Hadley Circulation over East Africa (35°E -40°E) (Fig. 2c). The east-west circulation was computed using the magnitude of zonal winds (u) and negative omega ($-\omega$). Figure 2a illustrates the intense upward motion caused by the Saharan thermal heating and Arabian thermal heating along the ITF. Warm air is lifted into the mid-troposphere, in which it will converge with the sinking cooler air from the upper-troposphere. The strong divergence from the vertical flow can be seen at the mid-troposphere located between 600 and 400 mb in West Africa and 600 to 500 mb in East Africa. This indicates that the Arabian high is shallower in comparison to the Saharan high. Similar divergent flows can be found on meridional cross sections averaged between 10°W to 15°W (Fig. 2b) and 35°E to 40°E (Fig. 2c). Figure 2b is a vertical cross section over the Saharan thermal low and Fig. 2c is a vertical cross section over the Arabian thermal low. Figures 2b and 2c are the magnitude of meridional winds (v) and negative omega ($-\omega$). The ITCZ is located between the southern Hadley Cell (south of 10°N) and the northern Hadley Cell (north of 10°N) with divergent flow in the upper troposphere. This is consistent with Chen's (2005) findings on the divergent flow from the northern and southern Hadley Cell interaction. The cross section in Fig. 2c reveals similarities of a divergent flow present in the upper-troposphere. There exists a Hadley Cell to the north and south of the ITCZ in the eastern African region. The ITF in East Africa starts in the lower troposphere around 20°N, and then tilts to the south around 12°N in the mid-troposphere where the strongest vertical motions are located.

4.2 Characteristics and Formation of the LWM_E and LWM_W

In the literature, the anticyclonic systems have been presented using streamfunction to show circulation. Simply taking the negative meridional gradient of streamfunction (not shown) will result in zonal wind with near real zonal wind estimations for the AEJ. In this study, we want to show how close the zonal geostrophic winds are to real zonal wind using the thermal wind relationship since understanding of it will help distinguish the differences of the LWM_E and the LWM_W.

The baroclinicity is strong in West Africa, East Africa and the Arabian Peninsula (Fig. 3a), but the LWM_E is weaker and smaller than the LWM_W. This raises the question we want to address: Why is the LWM_E weaker than the LWM_W? We hypothesize that the intensity of the weak LWM_E is caused by a weak mid-tropospheric high. Figure 3b illustrates the connection with the geostrophic wind maxima, which are associated with the Saharan high and Arabian high induced meridional geopotential gradients, respectively. The LWMs are located around 600 and 550 mb directly over the zonal geostrophic maxima in West Africa and East Africa. Since the Saharan high is more intense and broader than the Arabian high, the Saharan high produces a much stronger meridional geopotential gradient in West Africa, thus the making the LWM_W stronger than the LWM_E. The AEJ will be formed at 600 mb with an elongated easterly zonal geostrophic flow generated from baroclinicity. The presence of the Saharan and Arabian highs will increase easterly flow to the south of the anticyclonic centers because of the increased meridional geopotential gradient. This geopotential gradient along with the dominant influence from baroclinicity helps give the AEJ two distinct zonal maxima in East and West North Africa.

The local easterly zonal wind extends into the Arabian Peninsula along with a strong meridional temperature gradient, but a weakened meridional geopotential gradient. There is no LWM present over the Arabian Peninsula region. The AEJ decreases in intensity as a result of the meridional geopotential gradient decreasing, but the meridional temperature gradient remains intense across the southern Arabian Peninsula primarily because of the land-sea temperature contrast.

4. CONCLUSION

The African Easterly Jet was analyzed for the month of August between 1976 and 2010 to demonstrate a second maximum core located in East Africa centered around (15^oN, 35^oE). The LWM_E is located south of the Arabian high much like the LWM_W located south of the Saharan high. The increased intensity of the LWMs associated with AEJ is due to the maximum meridional geopotential gradient from the Saharan and Arabian highs, which causes the AEJ to be mainly geostrophic.

The formation and maintenance of the Saharan and Arabian highs were also discussed. From the east-west circulation, there were two distinct divergence flows in the mid-levels that were over Africa and the Arabian Peninsula. The upward vertical motion is associated with the ITF heating in which the Saharan and the Arabian thermal lows are located. The rising of warm air converges with the sinking cooler air forming divergence centers over Africa and the Arabian Peninsula. This differential heating from the divergent centers help maintain the anticyclones.

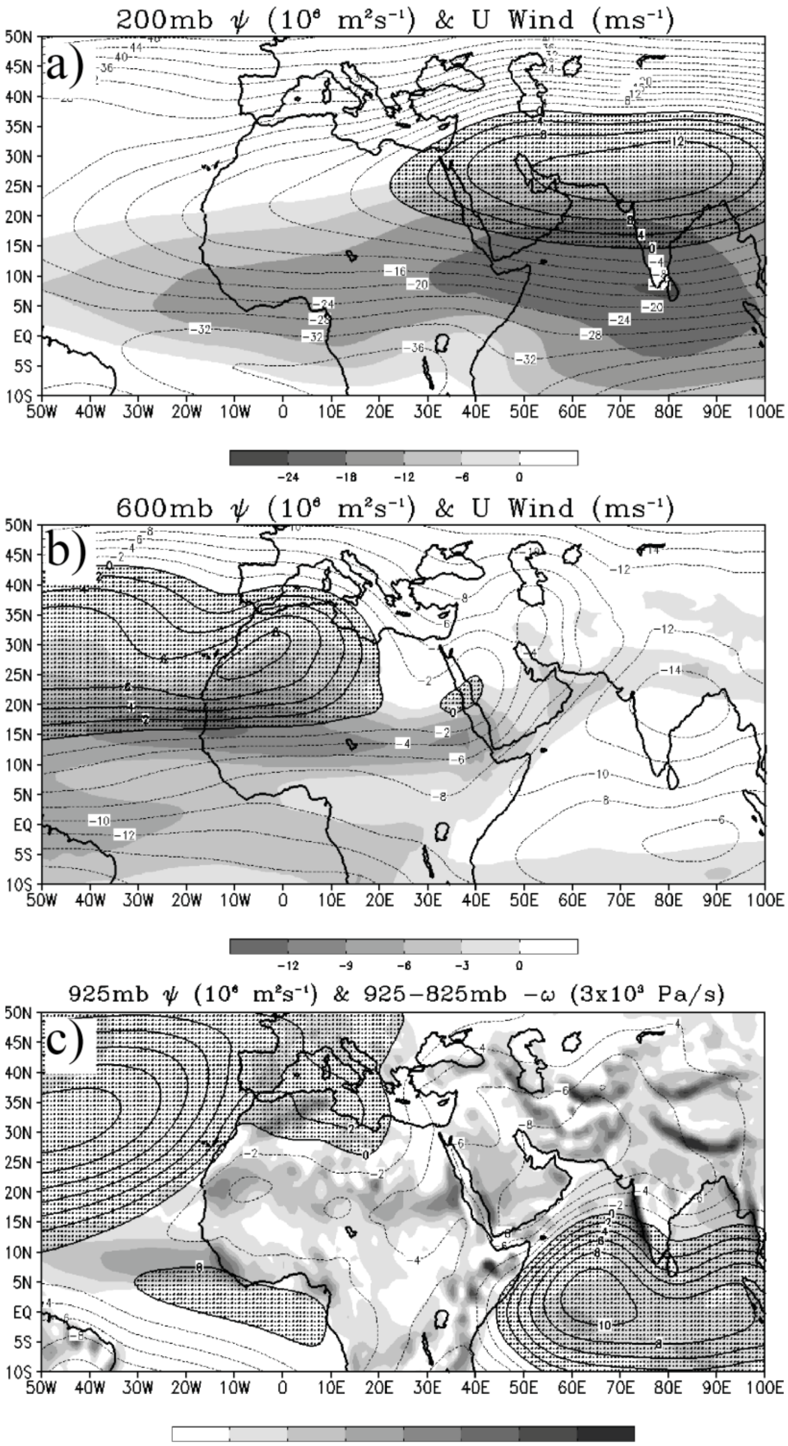

Figure 1: August 32-year (1979 – 2010) average of (a) 200 mb streamfunction (ψ) (x 10^6 m^2 s^{-1}) contoured every 2 m^2 s^{-1} and zonal velocity shaded every 6 m s^{-1}, (b) 600 mb streamfunction contoured every 2 m^2 s^{-1} and zonal velocity shaded every 3 m s^{-1}, and, (c) 925 mb streamfunction contoured every 2 m^2 s^{-1} and averaged 925-825 mb vertical velocity ($3x10^3$ Pa s^{-1}) shaded every 10 Pa s^{-1}.

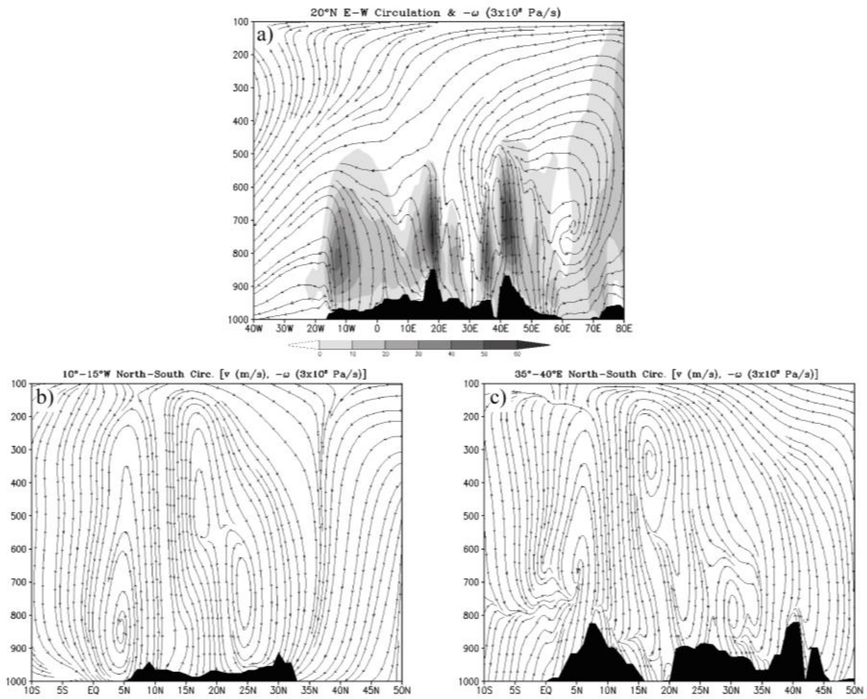

Figure 2: August 32-year (1979 – 2010) average of (a) zonal vertical cross section at 20°N of u and $-\omega$ (3 x 10^2 Pa s^{-1}), (b) meridional vertical cross section of v (m s^{-1}) and $-\omega$ (3 x 10^2 Pa s^{-1}) along 10°W – 15°W and (c) meridional vertical cross section along 35°E – 40°E of v (m s^{-1}) and $-\omega$ (3 x 10^2 Pa s^{-1}).

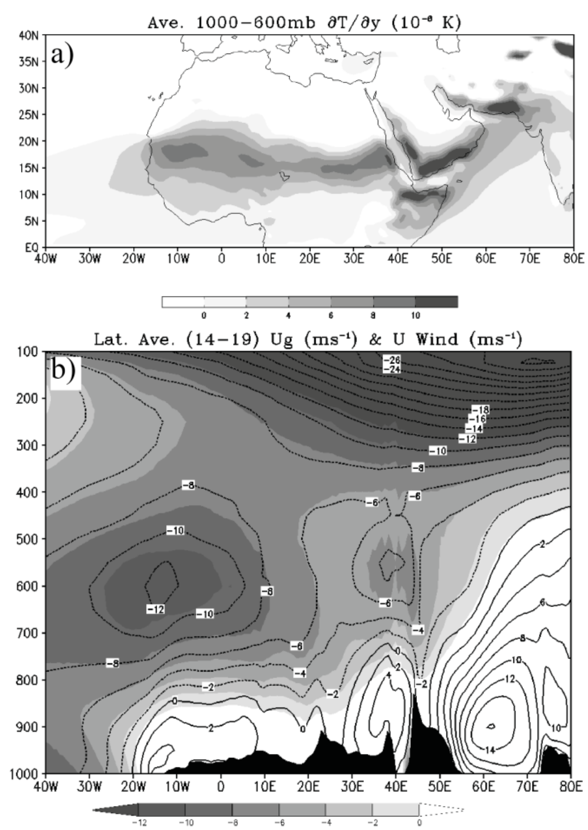

Figure 3: August 32-year (1979 – 2010) average of (a) the meridional temperature gradient (10^{-4} K) averaged between 1000 to 600 mb shaded every 2 K starting at 0 and meridional geopotential gradient contoured every 1 gmp starting at 0 and (b) vertical cross section between 14°N and 19°N of geostrophic wind (m s^{-1}) shaded every -2 m s^{-1} starting at 0 and zonal wind (m s^{-1}) contoured every 2 m s^{-1}. The terrain is crossed at 16°N.

References

Chen, T.-C., 2005: Maintenance of the midtropospheric North African summer circulation: Saharan high and African easterly jet. *J. Climate*., **18**, 2943 - 2962.

Cornforth, R. J., B. J. Hoskins, C. D. Thorncroft, 2009: Impact of moist processes on the African Easterly Jet-African Easterly Waves system. *Ouart. J. Roy. Meteor. Soc*., **135**, 894-913.

Cook, K. H., 1999: Generation of the African Easterly Jet and Its Role in Determining West African Precipitation. *J. Climate*, **12**, 1165 - 1184.

Dee, D. P. et al., 2011: The ERA-Interim reanalysis: configuration and performance of the data assimilation system. *Quart. J. Roy. Meteor. Soc*., **137**, 553 - 597.

Dezfuli, A. K., and S. E. Nicholson, 2010: A note on long term variations of the African easterly jet. *Int. J. Climatol.*, **31**, 2049 - 2054. doi: 10.1002/joc.2209.

Grist, J. P., S. E. Nicholson, and A. L. Barcilon, 2002: Easterly wave over Africa. Part II: Observed and modeled contrast between wet and dry years. *Mon. Wea. Rev*., **130**, 212 - 225.

Parker, D. J., C. D. Thorncroft, R.R. Burton, A. Diongue-Niang, 2005: Analysis of the African easterly jet using aircraft observations from the JET2000 experiment. *Quart. J. Roy. Meteor. Soc*, **131**(608): 1461 - 1482.

Reed, R. J., D. C. Norquist, and E. E. Recker, 1977: The structure and properties of African wave disturbances as observed during Phase III of GATE. *Mon. Wea. Rev*., **105**, 317 - 333.

Thorncroft, C. D., and M. Blackburn, 1999: Maintenance of the African easterly jet. *Quart. J. Roy. Meteor. Soc*., **125,** 763 - 786.

Thorncroft, C. D., D. J. Parker, R. R. Burton, M. Diop, J. H. Ayers, H. Barjat, S. Devereau, A. Diongue, R. Dumelow, D. R. Kindred, N. M. Price, M. Saloum, C. M. Tayor, and A.M. Tompkins: The Jet2000 Project: Aircraft observations of the African easterly jet and African easterly waves. *Bull. Amer. Meteor. Soc*., **84**, 337 - 351.